Title

Skeletogenic Capacity of Human Perivascular Stem Cells Obtained Via Magnetic-Activated Cell Sorting

Journal

Tissue Engineering Part A, 25(23-24)

ISSN

1937-3341

Authors

Meyers, Carolyn A
Xu, Jiajia
Zhang, Leititia
et al.

Publication Date

2019-12-01

DOI

10.1089/ten.tea.2019.0031

Peer reviewed

TISSUE ENGINEERING: Part A
Volume 25, Numbers 23 and 24, 2019

DOI: 10.1089/ten.tea.2019.0031

termis
Tissue Engineering
& Regenerative Medicine
International Society

ORIGINAL ARTICLE

Skeletogenic Capacity of Human Perivascular Stem Cells Obtained Via Magnetic-Activated Cell Sorting

Carolyn A. Meyers, BS,[1] Jiajia Xu, PhD,[1] Leititia Zhang, MD,[1,2] Leslie Chang, BS,[1] Yiyun Wang, PhD,[1] Greg Asatrian, DDS,[3] Catherine Ding, BA,[3] Noah Yan,[1] Erin Zou,[1] Kristen Broderick, MD,[4] Min Lee, PhD,[5] Bruno Peault, PhD,[3,6] and Aaron W. James, MD, PhD[1,3]

Human perivascular stem/stromal cells (PSC) are a multipotent mesenchymal progenitor cell population defined by their perivascular residence. PSC are increasingly studied for their application in skeletal regenerative medicine. PSC from subcutaneous white adipose tissue are most commonly isolated via fluorescence-activated cell sorting (FACS), and defined as a bipartite population of $CD146^{+}CD34^{-}CD31^{-}CD45^{-}$ pericytes and $CD34^{+}CD146^{-}CD31^{-}CD45^{-}$ adventitial cells. FACS poses several challenges for clinical translation, including requirements for facilities, equipment, and personnel. The purpose of this study is to identify if magnetic-activated cell sorting (MACS) is a feasible method to derive PSC, and to determine if MACS-derived PSC are comparable to our previous experience with FACS-derived PSC. In brief, $CD146^{+}$ pericytes and $CD34^{+}$ adventitial cells were enriched from human lipoaspirate using a multistep column approach. Next, cell identity and purity were analyzed by flow cytometry. *In vitro* multilineage differentiation studies were performed with MACS-defined PSC subsets. Finally, *in vivo* application was performed in nonhealing calvarial bone defects in *Scid* mice. Results showed that human $CD146^{+}$ pericytes and $CD34^{+}$ adventitial cells may be enriched by MACS, with defined purity, anticipated cell surface marker expression, and capacity for multilineage differentiation. *In vivo*, MACS-derived PSC induce ossification of bone defects. These data document the feasibility of a MACS approach for the enrichment and application of PSC in the field of tissue engineering and regenerative medicine.

Keywords: mesenchymal stromal cell, mesenchymal stem cell, bone tissue engineering, bone regeneration, magnetic activated cell sorting, MACS

Impact Statement

Our findings suggest that perivascular stem/stromal cells, and in particular adventitial cells, may be isolated by magnetic-activated cell sorting and applied as an uncultured autologous stem cell therapy in a same-day setting for bone defect repair.

Introduction

Perivascular cells and their possible functions were first described nearly 150 years ago by Charles-Marie Benjamin Rouget.[1–3] In 1923, Zimmerman first described the morphological features and functional contractility of pericytes.[4] Since this time, the progenitor cell attributes of vascular wall-resident mesenchymal cells have been well established.[5] Their ability to undergo differentiation to multiple cell lineages was later described by scattered observations from multiple investigators[6–8] such as Covas *et al.* who demonstrated the trilineage differentiation potential of mesenchymal stem/stromal cell (MSC)-like cells within human saphenous veins.[9] In 2008, Crisan *et al.* used a combination

[1]Department of Pathology, Johns Hopkins University, Baltimore, Maryland.
[2]Department of Oral and Maxillofacial Surgery, School of Stomatology, China Medical University, Shenyang, Liaoning Province, P.R. China.
[3]UCLA and Orthopaedic Hospital Department of Orthopaedic Surgery and the Orthopaedic Hospital Research Center, Los Angeles, California.
[4]Department of Surgery, Johns Hopkins University, Baltimore, Maryland.
[5]School of Dentistry, University of California, Los Angeles, California.
[6]Center For Cardiovascular Science and MRC Center for Regenerative Medicine, University of Edinburgh, Edinburgh, United Kingdom.

of immunohistochemical and flow cytometry analysis on perivascular stem/stromal cells (PSC), allowing their multipotent mesenchymal progenitor cell identity to be fully appreciated.[10] Since then, multiple independent investigators have confirmed the progenitor cell attributes of perivascular cells (see[5] for a review), and several groups have identified pericytes as progenitor cells involved in endogenous tissue repair.[8,11–14] In summary, multiple investigators have defined the perivascular residence of mesenchymal progenitor cells in diverse tissues.

Adipose-derived MSCs have been studied extensively for preclinical use in tissue engineering (reviewed in[15]) for their advantages as a source of multilineage stromal cells,[16] high rate of cell proliferation, potential for osteogenic differentiation, and low donor site morbidity. Because the stromal vascular fraction (SVF) of adipose tissue is highly heterogeneous and composed of perivascular, inflammatory, endothelial, and other stromal cells, fluorescence-activated cell sorting (FACS) may be used to purify adipose-derived stromal cell populations. This cell sorting approach has previously resulted in some success in enriching ''osteoprogenitor''[17] or ''chondroprogenitor''[18] cell types, but not in the isolation of multipotent mesenchymal progenitor cells. Our research group has extensively validated the use of FACS for the derivation of cells within the perivascular niche, termed PSC,[19] which are abundant in adipose tissue.[20,21] PSC are composed of two related cell populations[5,10] that are distinguished by location within the vessel wall, transcriptome, and antigen expression, including pericytes ($CD146^+CD34^-CD31^-CD45^-$) and adventitial cells ($CD34^+CD146^-CD31^-CD45^-$).[10,22] Additional characteristic cell surface marker of PSC include those canonical markers of mesenchymal progenitor cells, such as CD44, CD73, CD90, and CD105.[19]

As an uncultured cellular therapy, adipose tissue-derived PSC have significant potential for use in skeletal tissue engineering, with efficacy in intramuscular,[21,23] spinal fusion,[20,23] and calvarial defect models.[24] This lies in contrast to the SVF of adipose tissue, which has modest[24] or unreliable[25] bone forming effects. In particular, Saxer *et al.* examined the efficacy of autologous SVF as a treatment for low-energy fracture repair both in preclinical and clinical studies.[25] In both experiments, SVF cells were combined with ceramic granules and fibrin hydrogel, then implanted into the void space of the fracture.[25] In the preclinical rat femoral segmental defect model, histological analysis revealed that although all explants showed some signs of preosteoid formation, only five out of the nine SVF-loaded constructs generated newly formed bone inside of the ceramic pores.[25] In the clinical trial, 8 human patients older than the age of 50 participated in a clinical study using autologous SVF cell-based constructs for augmentation of fractures of the proximal humerus. Although bone formation and angiogenesis were observed in most patients, the results were somewhat unreliable, as the SVF led to variable bone formation (including a patient who formed no new bone) and had variable CFU formation (up to 42-fold different CFU forming ability) and clonal osteoblast formation (ranging from 0 to 17 osteoblastic colonies) in culture.[25] These studies point to the inherent variability in SVF, and raise the possibility that a more purified stromal population could represent a major advance for clinical translation.

Despite its feasibility in a laboratory setting, FACS poses challenges for clinical translation, including requirements for specialized facilities, equipment, and personnel.[26] Magnetic-activated cell sorting (MACS) is a simpler alternative, which uses biodegradable paramagnetic nanobeads for cell enrichment. MACS is commonly used for cell enrichment for its speed and ease of use relative to other more complex separation strategies. While isolation of FACS-derived PSC requires skilled personnel and a separate facility with specialized equipment, MACS-derived PSC can be isolated in a simpler procedure in an on-site clean room by personnel with less advanced training. Since PSC are abundant in human adipose tissue in clinically relevant numbers, there is no need for culture expansion of cells before application. Therefore, MACS could be performed in 1–2 h and PSC could be theoretically applied the same day. This same-day approach has been previously published in experimental animal models with FACS-derived PSC.[21] In addition, MACS isolation tends to be gentler on cells than other cell separation methods. Specifically, during FACS sorting, cells are exposed to hydrodynamic stress, which can lead to cell damage.[27,28] Physical damage that can occur includes damage to cell surface antigens and loss of plasma membrane integrity.[28] In addition, cells subjected to FACS are prone to oxidative stress and metabolic changes.[29,30] For example, in a study comparing MACS- and FACS-sorted bone marrow stromal cells (BMSCs) from Sprague-Dawley rats, FACS-sorted cells had lower viability and experienced reduced chemotactic migration.[31] In addition, unlike some other column-free methods of cell isolation, the strong magnetic field used in MACS technology allows for minimal labeling, resulting in separation of cells free of aggregates, epitope blocking, and cross-linking. Importantly, MACS is scalable and also has the option to be implemented with automated equipment and in large quantities for use in a clinical setting. Columns can also be used in sequence for complicated isolations or to further enhance purity. In the current study, we sought to validate MACS-enriched PSC as a clinically translatable cell population for bone tissue engineering.

Materials and Methods

PSC immunolocalization

Human adipose tissue was obtained under Johns Hopkins University Institutional Review Board (JHU IRB) approval, and flash frozen in optimal cutting temperature compound. Tissues were sectioned at 30 μm and fixed with ice-cold acetone. Blocking was performed with 10% normal goat serum. Anti-CD34-APC and anti-CD146-FITC (Supplementary Table S1) were then added overnight at 4°C (1:100). Images were obtained on a Zeiss 780 confocal microscope.

MACS enrichment and analysis

Lipoaspirate from healthy adult patients was obtained from cosmetic liposuction procedures under IRB approval. Lipoaspirate from $n = 3$ biological replicates was digested in 1 mg/mL collagenase II (CLS-2; Worthington Biochemical) for 45 min at 37°C in a shaking water bath at 100 rpm, centrifuged at 2000 rpm for 10 min. The digest was filtered sequentially through 100 and 40 μM strainers. All products

used in MACS enrichment were obtained from Miltenyi Biotec (Supplementary Table S2). Depletion of endothelial and inflammatory cells was achieved using anti-CD31 and anti-CD45 microbeads with an LS column using a MidiMACS separator. Next, sequential positive selection was performed using anti-CD34 and anti-CD146 microbeads. Purity and cell yield were assessed by flow cytometry on a FACSCanto sorter using freshly purified, uncultured cells. Antibodies were used at a 1:100 dilution per 1×10^6 cells (Supplementary Table S1).

Differentiation assays

For all differentiation assays, MACS-derived PSC passages 1–4 were used. PSC were seeded in 24-well plates at a density of 2×10^4 cells/well and cultured under osteogenic or adipogenic differentiation conditions.[32] Osteogenesis was assessed by alkaline phosphatase (ALP) and Alizarin red staining and specific gene expression by quantitative real-time polymerase chain reaction (qRT-PCR) over 10 days.[32] Osteogenic gene marker expression was assessed by qRT-PCR, including runt-related transcription factor 2 *(RUNX2)*, osteopontin (*OPN*), and osterix *(OSX)* at sequential timepoints after osteogenic differentiation. Adipogenesis was assessed by oil red O (ORO) staining and qRT-PCR over 10 days.[32] Adipogenic gene marker expression by qRT-PCR, including CCAAT/enhancer-binding protein α *(CEBPα)*, lipoprotein lipase *(LPL)*, fatty acid-binding protein 4 *(FABP4)*, and peroxisome proliferator-activated nuclear receptor γ *(PPARγ)*, was assessed at sequential timepoints after adipogenic differentiation. Chondrogenic differentiation was performed in micromass (200,000 cells in 10 μL) over 21 days,[33] with assessments by Alcian Blue and Safranin O staining and qRT-PCR.[33] Expression of the chondrogenic differentiation marker, collagen type 2 *(COL2)*, was assessed in micromass culture at sequential timepoints after chondrogenic differentiation.

Ribonucleic acid and qRT-PCR

Gene expression was assayed by qRT-PCR, based on our previous methods.[34,35] Time points for specific gene expression include 0, 3, 7, and 10 days for the analysis of osteogenic and adipogenic markers, and 7, 14, and 21 days for the analysis of chondrogenic markers. In brief, total RNA was extracted using the RNeasy Kit (Qiagen, Santa Clarita, CA). One microgram of total RNA from each sample was then subjected to first-strand complementary DNA (cDNA) synthesis using the iScript cDNA Synthesis Kit (Bio-Rad, Hercules, CA) to a final volume of 20 μL. The reverse transcription reaction was performed using SYBR green qPCR master mix (Applied Biosystems, Foster City CA) at 25°C for 5 min, 46°C for 20 min, and 95°C for 1 min. qRT-PCR were run using the CFX96 Real-Time PCR detection system (Bio-Rad). Reactions were incubated in 96-well optical plates at 95°C for 10 min, followed by 40 cycles at 95°C for 15 s, and at 60°C for 60 s. The threshold cycle (Ct) data were determined using default threshold settings. The Ct was defined as the fractional cycle number at which the fluorescence passes the fixed threshold. Reactions were run in triplicate per RNA isolate and compared to the housekeeping gene, *β-actin* (*ACTB*). Primer sequences are in Supplementary Table S3.

Surgical procedures

Twelve-week-old male C57/BL6 *Scid* mice were used (Supplementary Table S4). 4.0 mm circular defects were created in the parietal bone using an Ideal Micro-Drill and a burr (Xemax Surgical, Napa Valley, CA).[36] Hydroxyapatite-coated poly(lactic-co-glycolic acid) scaffolds were fabricated to fit the defect size (4.0 mm diameter, 0.5 mm thickness).[37] Culture-expanded $CD34^+$ adventitial cells (passages 5–6) were seeded onto the scaffold. Scaffolds were preincubated in 96-well plates (250,000 cells/scaffold) overnight for adherence before application, or preincubated for a further 3 days in osteogenic differentiation medium (ODM). Scaffolds, with or without cells, were rinsed with PBS and applied to parietal bone defects. After eight weeks, microcomputed tomography (microCT) reconstruction and analyses were performed.[36]

Statistical analysis

Quantitative data are expressed at mean ± standard error of the mean. A Shapiro–Wilk test for normality was performed on all datasets. Homogeneity was confirmed by a comparison of variances test. Parametric data were analyzed using a one-way analysis of variance, followed by a *post hoc* Tukey's test to compare two groups. Nonparametric data were analyzed with a Kruskal–Wallis one-way analysis when more than two groups were compared.

Results

Human adipose PSC isolation via MACS

First, PSC were identified *in situ* by characteristic expression of CD34 within progenitors of the tunica adventitia (red) (Fig. 1A) and expression of CD146 in pericytes within the tunica intima of small caliber vessels (green) (Fig. 1B). To validate a magnetic microbead-based approach to adipose tissue PSC derivation, a multistep approach was taken (Fig. 1C). First, $CD45^+$ inflammatory cell and $CD31^+$ endothelial cell depletion was performed, representing 38.33% (±1 SD:7.49%) of total mononuclear SVF (Table 1). $CD34^+CD31^-CD45^-$ adventitial cells were next isolated, representing on average 18.19% (±1 SD:3.37%) of total SVF. Next, $CD146^+CD34^-CD31^-CD45^-$ pericytes were isolated, representing 1.87% (±1 SD:0.90%) of total SVF. Cell purity among uncultured, MACS-defined adventitial cells and pericytes was assessed by flow cytometry, interrogating for frequency of CD146, CD34, CD31, and CD45 expressing cells (Fig. 2A–C, Supplementary Fig. S1). A small endothelial cell contaminant was observed among both $CD34^+$ adventitial cells (0.26% $CD31^+$ cells, Fig. 2B) and $CD146^+$ pericytes (4.64% $CD31^+$ cells, Supplementary Fig. S1B). A minor inflammatory cell contaminant was observed among both $CD34^+$ adventitial cells (9.38% $CD45^+$ cells, Fig. 2C) and $CD146^+$ pericytes (21.76% $CD45^+$ cells, Supplementary Fig. S1C). After four passages of culture expansion, virtually no endothelial or hematopoietic contaminant remained (up to 0.1% $CD31^+$ and 0.08% $CD45^+$ cells, *data not shown*). Canonical mesenchymal progenitor cell markers were highly expressed among PSC subsets, including CD44, CD73, CD90, and CD105 (Fig. 2D–G).

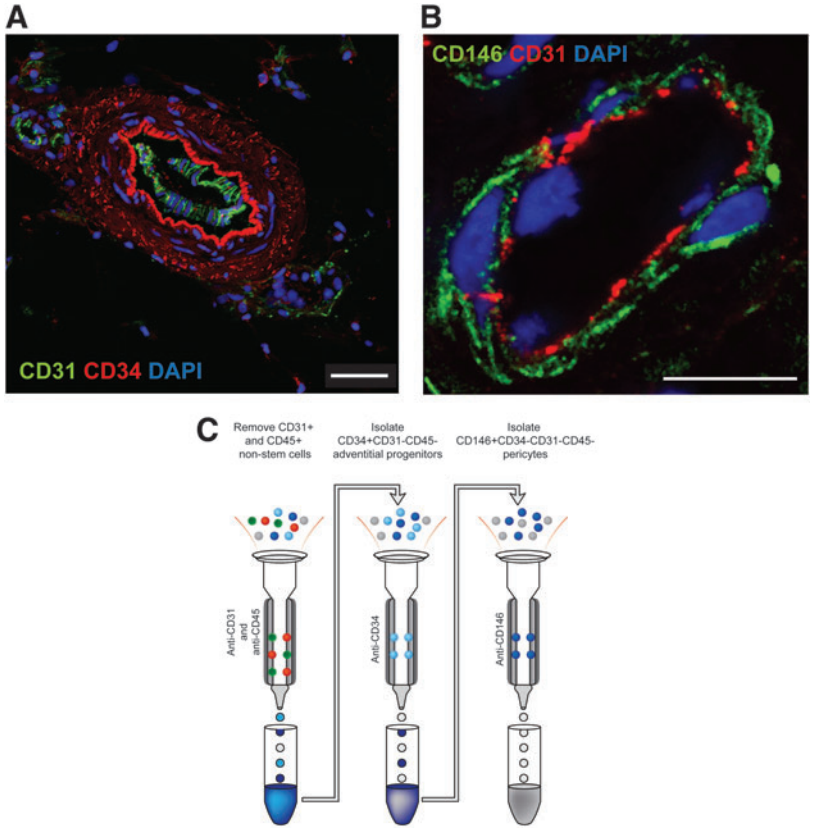

FIG. 1. PSC location in human adipose tissue and MACS purification scheme from human lipoaspirate. **(A)** A larger caliber artery within human adipose tissue, examined in a cross-section using confocal microscopy. CD34 immunostaining (*red*) highlights characteristic $CD34^+$ adventitial cells within the tunica adventitia. CD31 immunostaining (*green*) highlights the endothelium. Scale bar = 50 μm **(B)** A smaller caliber vessel within the same section of human adipose tissue, examined in cross-section using confocal microscopy. CD146 immunostaining (*green*) highlights characteristic $CD146^+$ pericytes within the tunica intima. CD31 immunostaining (*red*) highlights the endothelium. Scale bar = 10 μm. **(C)** Schematic of MACS isolation of human PSC from the SVF of adipose tissue (*left*). Anti-CD31 and anti-CD45 microbeads are used in a depletion column to remove endothelial and inflammatory cells, respectively. The flowthrough is saved for further purification (*center*). Next, the $CD31^-CD45^-$ flowthrough cells are incubated with anti-CD34 microbeads and adventitial cells are collected as a $CD34^+CD31^-CD45^-$ cell population (*right*). The $CD34^-CD31^-CD45^-$ flowthrough from the *center column* is next incubated with anti-CD146 microbeads and passed through a third column (*right*) to collect $CD146^+CD34^-CD31^-CD45^-$ pericytes. MACS-derived cells are either used for flow cytometry analysis, *in vitro* expansion, or *in vivo* application. MACS, magnetic activated cell sorting; PSC, perivascular stem/stromal cells; SVF, stromal vascular fraction. Color images are available online.

Multilineage differentiation of MACS-defined PSC

Trilineage differentiation potential of MACS-defined PSC subsets was next examined (Fig. 3, Supplementary Fig. S2). Both MACS-defined adventitial cells and pericytes demonstrated lipid accumulation and increasing adipocytes-specific gene expression under appropriate conditions (Fig. 3A, B Supplementary Fig. S2A, B). Osteogenic differentiation among MACS-derived PSC subsets was observed by ALP activity, bone nodule deposition, and temporal changes in osteoblast-specific gene expression (Fig. 3C–E, Supplementary Fig. S2C, D). In high-density micromass culture, MACS-defined PSC subsets likewise showed an increase in Alcian Blue and Safranin O staining, as well as *COL2* gene expression (Fig. 3F–H, Supplementary Fig. S2E, F).

Bone healing with MACS-defined PSC

The bone healing potential of MACS-defined adventitial cells was next assessed using a xenotransplant of $CD34^+$ adventitial cells in a nonhealing mouse parietal bone defect (Fig. 4). MACS-defined $CD34^+$ adventitial cells were seeded on polymeric scaffolds and implanted after overnight incubation, or left for three days in ODM before implantation. MicroCT imaging and analysis demonstrated a significant increase in osseous repair by all metrics with MACS-defined $CD34^+$ cell treatment.

Discussion

MACS technology is currently used in a wide variety of clinical applications for tissue engineering, including purification of heart cells for cardiac tissue engineering,[38] isolation, and cultivation of neurons and other populations from the central nervous system,[39] purification of skeletal muscle precursor cells,[40] isolation of endothelial cells for engineering vascularized tissue surrogates,[41] and isolation of putative MSC.[42,43] In the current study, we used MACS technology to isolate $CD34^+$ and $CD146^+$ perivascular progenitor cells to

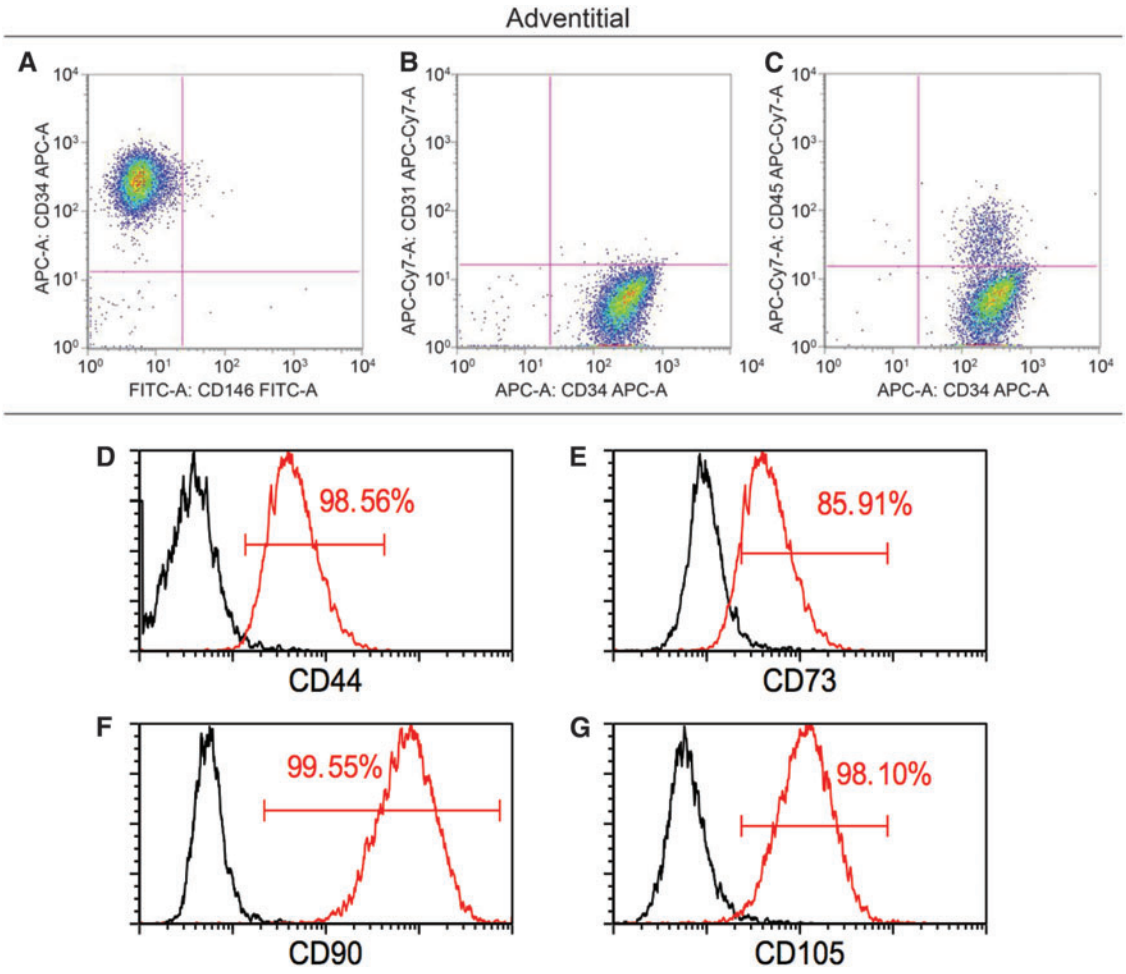

FIG. 2. Purity and MSC marker expression in MACS-defined $CD34^+$ adventitial cells. Adventitial cells are isolated after CD31 and CD45 depletion, by incubation with anti-CD34 microbeads and capture of magnetically labeled $CD34^+$ cells. **(A–C)** Flow cytometry analysis of freshly derived adventitial cells. **(A)** Virtually all cells are $CD34^+CD146^-$ (98.7%), while a subset is $CD34^+CD146^+$ (1.16%). **(B)** Virtually all cells are $CD34^+CD31^-$ (99.27%), while a subset is $CD34^+CD31^+$ (0.26%). **(C)** The majority of cells are $CD34^+CD45^-$ (90.45%), while a subset of cells is $CD34^+CD45^+$ (9.38%). **(D–G)** Canonical MSC marker expression among freshly isolated and MACS-defined $CD34^+CD146^-CD31^-CD45^-$ adventitial cells. Canonical MSC markers are expressed at high frequency in MACS-defined adventitial cells, including **(D)** CD44 (98.56%), **(E)** CD73 (85.91%), **(F)** CD90 (99.55%), and **(G)** CD105 (98.10%). Data shown as overlaid histograms with stained MACS-defined adventitial progenitor cells in *red* in comparison to unstained controls in *black*. Representative data shown, repeated in biologic triplicate. MSC, mesenchymal stem/stromal cell. Color images are available online.

confirm their ability to undergo trilineage differentiation, as well as their potential for applications in bone tissue regeneration.

Traditional methods for separating progenitor cells include density gradient centrifugation, differential adhesion, and culturing in selective serum-containing media.[44] However, these methods are largely nonspecific and result in cultures with low purity. Alternatively, improved isolation methods that are commonly used include the usage of fluorescent antibodies (FACS) or magnetic beads (MACS) to enrich for specific cell surface antigens. Although the current study did not directly compare MACS-derived PSC to FACS-derived PSC, the current study serves as a logical extension of our previous work. We have previously analyzed FACS-derived PSC and described this population in detail in several publications in comparison to unpurified lipoaspirate-derived SVF.[20,21,23,24,45,46] For example, in an intramuscular implant model, FACS-derived PSC were compared to patient-matched SVF.[21] Equal numbers of PSC were found to lead to significantly greater ectopic bone formation by radiographic and histologic endpoints. In a subsequent study, and in a *Scid* mouse calvarial defect model, FACS-derived PSC were compared to patient-matched SVF. Here, FACS-derived PSC again led to greater bone formation and defect reossification than an unpurified adipose-derived cell therapy.[24] Analogous studies have been recapitulated in an athymic rat spine fusion model,[19] although the comparison to unsorted SVF is unpublished. Here, FACS-derived PSC led to a 100% rate of spine fusion as assessed by a manual palpation score. This lies in contrast to an $\sim$20% rate of spine fusion we have observed among human adipose-derived SVF treatment under equal conditions and cell seeding densities (*unpublished results*). Thus, our past comparisons of FACS-derived PSC to unpurified SVF suggest highly that an analogous MACS-

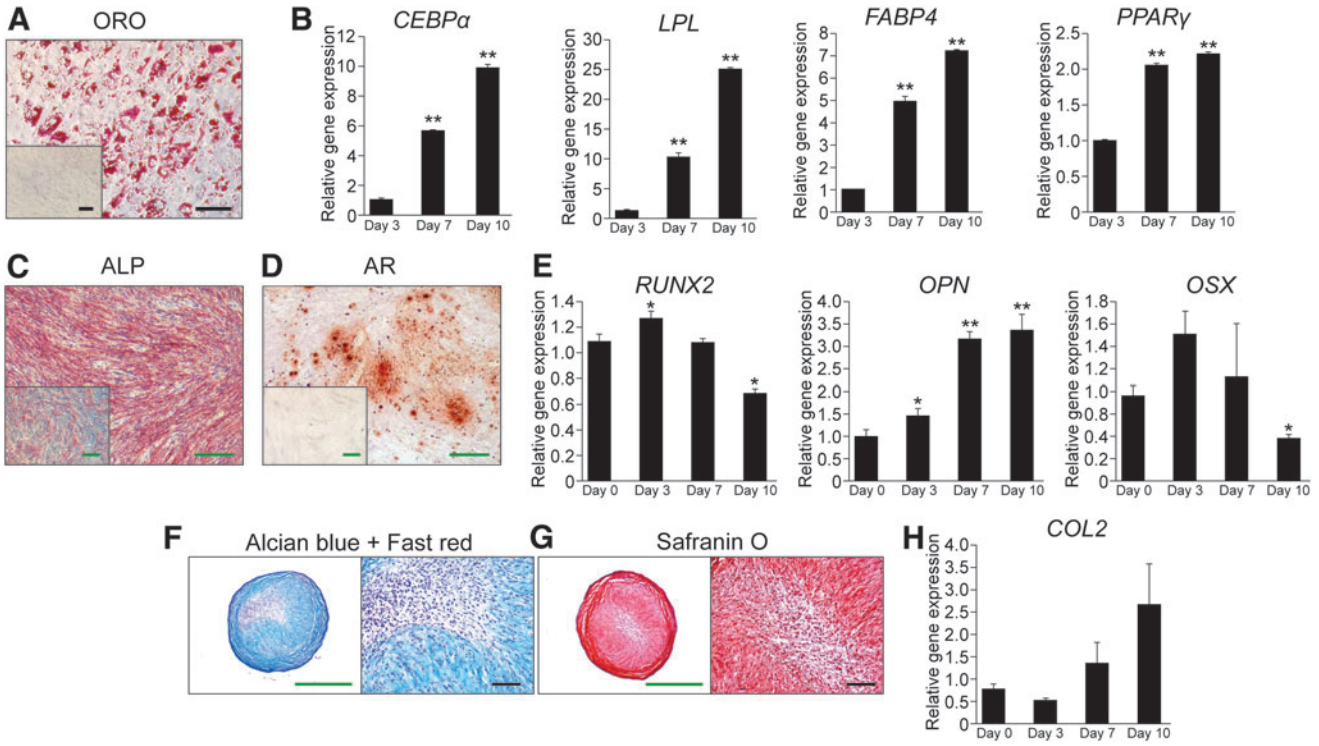

FIG. 3. Trilineage differentiation potential of MACS-defined CD34$^+$ adventitial cells. **(A, B)** Adipogenic differentiation of MACS-defined CD34$^+$ adventitial cells in monolayer. **(A)** ORO staining of intracellular lipid accumulation at day 10 of differentiation. *Inset* depicts standard growth medium (SGM) control. **(B)** Adipogenic gene marker expression by qRT-PCR, including *CEBPα*, *LPL*, *FABP4*, and *PPARγ*, at sequential timepoints after adipogenic differentiation. $^{**}p<0.01$ in comparison to day 3. **(C–E)** Osteogenic differentiation of MACS-defined CD34$^+$ adventitial cells in monolayer. **(C)** ALP activity at 5 days of differentiation. *Inset* depicts standard growth medium (SGM) control. **(D)** Alizarin *Red* (AR) staining of bone nodule formation at 10 days of differentiation. *Inset* depicts standard growth medium (SGM) control. **(E)** Osteogenic gene marker expression by qRT-PCR, including *RUNX2*, *OPN*, and *OSX* at sequential timepoints after osteogenic differentiation. $^{*}p<0.05$ and $^{**}p<0.01$ in comparison to day 0. **(F–H)** Chondrogenic differentiation of MACS-defined CD34$^+$ adventitial cells in 3D micromass. **(F)** Alcian Blue/fast red staining of micromass cross sections after 21 days differentiation. **(G)** Safranin O staining of micromass cross sections after 21 days differentiation. **(H)** Expression of the chondrogenic differentiation marker, *COL2*, in micromass culture as sequential timepoints after chondrogenic differentiation. *Black scale bar* = 50 μM. *Green scale bar* = 250 μM. Representative data shown, repeated in biologic triplicate. ALP, alkaline phosphatase; *CEBPα*, CCAAT/enhancer binding protein α; *COL2*, collagen type 2; *FABP4*, fatty acid-binding protein 4; LPL, lipoprotein lipase; *OPN*, osteopontin; *PPARγ,* peroxisome proliferator-activated nuclear receptor γ; ORO, oil red O; *OSX*, osterix; qRT-PCR, quantitative real-time polymerase chain reaction; *RUNX2*, runt-related transcription factor 2. Color images are available online.

derived PSC preparation would be of similar efficacy in bone regeneration.

However, important differences did exist between FACS- and MACS-derived human adipose tissue PSC. In comparison to FACS-derived PSC, MACS isolation overall had a lower total yield of cells, was in general more time consuming to perform, and most importantly left behind a greater number endothelial and inflammatory contaminants. Cell contaminants were not only greater in CD146$^+$ pericyte cell isolates (observed at a frequency of ~4.6% CD31$^+$ cells and ~21.8% CD45$^+$ cells) but also present in CD34$^+$ adventitial cell preparations (observed at a frequency of ~0.3% CD31$^+$ cells and ~9.4% CD45$^+$ cells). The role of endothelial cell contaminants and their potential interaction with mesenchymal progenitor cells during osteogenic differentiation has been previously studied. While some investigators have found that endothelial cells inhibit mesenchymal progenitor cell osteogenic differentiation in culture,[47] this result seems to be context dependent, as not all investigators have been able to reproduce this effect.[48–50] For example, Meury *et al.* found that in coculture conditions, human endothelial cells attenuate osteogenic differentiation of BMSCs by inhibiting *OSX* expression, ALP activity, and matrix mineralization.[47] However, other investigators have found that endothelial cells support osteoblastic function when cocultured with osteoprogenitor cells.[49] In particular, Guillotin *et al.* showed that the short-term effects of coculturing osteoprogenitor cells with endothelial supported the proliferation of osteoprogenitor cells without impairing their long-term ability to differentiate.[50] Similarly, Zhao *et al.* found that when cocultured with ASC, endothelial cells stimulated ALP activity and increased mineralization.[48] It is important to note that most of these coculture experiments used different variables, including the ratio of endothelial progenitor cells, and whether or not coculture was performed in contact or

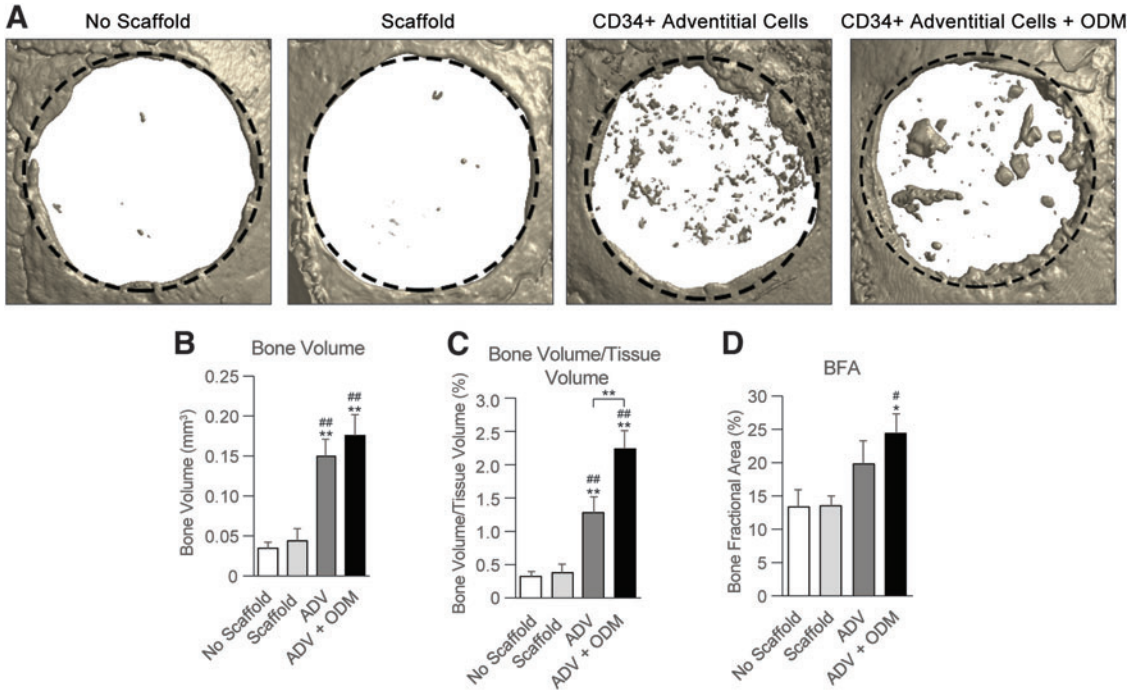

FIG. 4. Critical size mouse calvarial defect healing by MACS-defined $CD34^+$ adventitial cells. MACS-defined $CD34^+$ adventitial cells were applied to nonhealing, 4 mm circular calvarial defects within the parietal bone of *Scid* mice. Treatment groups included no scaffold control (empty defect), scaffold (acellular control, hydroxyapatite-coated PLGA scaffold), $CD34^+$ adventitial (ADV) cells without pretreatment, and $CD34^+$ adventitial cells with predifferentiation (3 day pulse of ODM before implantation, ADV+ODM). **(A)** Representative microCT reconstructions of bone defects, presented in a top down view eight weeks postinjury. The original defect size is indicated by a *dashed black circle* 4.0 mm in diameter. **(B)** Bone Volume and **(C)** Bone Volume/Tissue Volume of the treated bone defect sites, using CTAn microCT analysis software 80. **(D)** Bone fractional area (BFA) of the treated bone defects sites, determined using the fractional area of bone per original defect area using Adobe Photoshop cc. $*p<0.05$, $**p<0.01$ in comparison to no scaffold; $^{\#}p<0.05$, $^{\#\#}p<0.01$ in comparison to scaffold alone. microCT, microcomputed tomography; ODM, osteogenic differentiation medium; PLGA, poly(lactic-co-glycolic acid). Color images are available online.

noncontact conditions. In aggregate, it is not yet clear if an endothelial contaminant within MACS-derived PSC would have a deleterious effect on osteogenic differentiation *in vitro* or bone formation *in vivo*.

Prior reports have isolated perivascular cell types using magnetic cell sorting techniques from other tissues and species. For example, Tsang *et. al* showed that $CD146^+$ perivascular cells derived from human umbilical cord using Dynabeads induce mineralization in an ectopic bone formation model and a femoral defect model.[51] In a similar study, Wu *et al.* used MACS to isolate $CD146^+$ perivascular cells from the growth plates of from Sprague-Dawley rats for *in vitro* studies.[52] These $CD146^+$ cells were shown to have higher colony forming capacity and better *in vitro* chondrogenic differentiation potential than nonenriched cell fractions.[52] Although $CD34^+$ cell enrichment is well validated in hematopoietic stem cell biology and applications,[53–55] to our knowledge, this is the first report of MACS enrichment for $CD34^+$ adventitial cells.

In summary, MACS represents a clinically translatable method for PSC enrichment. Among PSC subsets, the $CD34^+$ adventitial cell population is most readily applicable for MACS derivation, as this more frequent cell population has lower cellular contaminants and similar frequency to FACS derivation. Based on this cell frequency, MACS-defined PSC would represent $\sim 5.4 \pm 0.6$ M (1 SD) cells per 100 mL human lipoaspirate, which is within the range of PSC yield from FACS in our previous studies in 131 samples [9.3 M ± 5.5 M (1 SD) cells per 100 mL human lipoaspirate][46]. Importantly, this represents clinically relevant numbers even for large-scale reconstructions. MACS-defined PSC subsets demonstrate the same conserved features of FACS-derived PSC, including canonical MSC marker expression, multilineage differentiation potential, and the ability to induce osseous repair. The low-frequency pericyte population ($CD146^+CD34^-CD31^-CD45^-$) exhibited a higher endothelial and hematopoietic contaminant among MACS preparations, although purity after culture

Table 1. Perivascular Stem/Stromal Cell Frequency via Magnetic-Activated Cell Sorting from Human Lipoaspirate

	% of total SVF	*% of $CD31^-$/$CD45^-$ cells*
$CD31^-/CD45^-$	38.33 ± 7.49	—
$CD31^-/CD45^-/CD34^+$	18.19 ± 3.37	47.84 ± 5.93
$CD31^-/CD45^-/CD34^-/CD146^+$	1.87 ± 0.90	4.86 ± 1.07

Average cell frequency, reported either as a percentage of total mononuclear SVF, or as a percentage of $CD31^-CD45^-$ cells. $n=3$ human lipoaspirate samples.

SVF, stromal vascular fraction.

expansion with either PSC subset was high. These findings suggest that PSC, and in particular adventitial cells, may be isolated by MACS and applied as an uncultured autologous stem cell therapy in a same-day setting for bone defect repair.

Acknowledgments

The present work was supported by the NIH/NIAMS (R01 AR070773, K08 AR068316, R21 DE027922, S10O D016374), Department of Defense (W81XWH-18-1-0121, W81XWH-18-1-0336, W81XWH-18-10613), American Cancer Society (132226-RSG-18-027-01), the Orthopaedic Research and Education Foundation with funding provided by the Musculoskeletal Transplant Foundation, the Maryland Stem Cell Research Foundation, and the Musculoskeletal Transplant Foundation. The content is solely the responsibility of the authors and does not necessarily represent the official views of the National Institute of Health or Department of Defense. We thank the JHU microscopy facility for their technical assistance.

Authors' Contributions

C.A.M.: Collection and assembly of data, article writing, data analysis, and interpretation; J.X.: Collection and assembly of data, data analysis, and interpretation; L.Z.: Collection and assembly of data, data analysis, and interpretation; L.C.: Collection and assembly of data; Y.W.: Collection and assembly of data; G.A.: Collection and assembly of data; C.D.: Collection and assembly of data; N.Y.: Collection and assembly of data; E.Z.: Collection and assembly of data; K.B.: provision of study materials; M.L.: provision of study materials; B.P.: conception and design; A.W.J.: conception and design, financial support, data analysis and interpretation, article writing, and final approval of article.

Disclosure Statement

B.P. is an inventor of perivascular stromal cell-related patents filed from UCLA.

Supplementary Material

Supplementary Figure S1
Supplementary Figure S2
Supplementary Table S1
Supplementary Table S2
Supplementary Table S3
Supplementary Table S4

References

1. Rouget, C. The contractility of blood capillaries (Fr). C R Acad Scu **88,** 916, 1879.
2. Rouget, C. Note on the development of the contractile walls of blood vessels (Fr.). C R Acad Sci **79,** 559, 1874.
3. Rouget, C. Memory on the development, structure and physiological properties of blood and lymphatic capillaries [in German]. Arch Physiol Norm Path **5,** 603, 1873.
4. Zimmerman, K. The finer construction of the blood capillaries [in French]. Z Anat Entwicklugsgesch **68,** 29, 1923.
5. Murray, I.R., West, C.C., Hardy, W.R., *et al.* Natural history of mesenchymal stem cells, from vessel walls to culture vessels. Cell Mol Life Sci **71,** 1353, 2014.
6. Collett, G.D., and Canfield, A.E. Angiogenesis and pericytes in the initiation of ectopic calcification. Circ Res **96,** 930, 2005.
7. Doherty, M.J., and Canfield, A.E. Gene expression during vascular pericyte differentiation. Crit Rev Eukaryot Gene Expr **9,** 1, 1999.
8. Farrington-Rock, C., Crofts, N.J., Doherty, M.J., Ashton, B.A., Griffin-Jones, C., and Canfield, A.E. Chondrogenic and adipogenic potential of microvascular pericytes. Circulation **110,** 2226, 2004.
9. Covas, D.T., Piccinato, C.E., Orellana, M.D., *et al.* Mesenchymal stem cells can be obtained from the human saphena vein. Exp Cell Res **309,** 340, 2005.
10. Crisan, M., Yap, S., Casteilla, L., *et al.* A perivascular origin for mesenchymal stem cells in multiple human organs. Cell Stem Cell **3,** 301, 2008.
11. Richardson, R.L., Hausman, G.J., and Campion, D.R. Response of pericytes to thermal lesion in the inguinal fat pad of 10-day-old rats. Acta Anat (Basel) **114,** 41, 1982.
12. Dore-Duffy, P., Owen, C., Balabanov, R., Murphy, S., Beaumont, T., and Rafols, J.A. Pericyte migration from the vascular wall in response to traumatic brain injury. Microvasc Res **60,** 55, 2000.
13. Zebardast, N., Lickorish, D., and Davies, J.E. Human umbilical cord perivascular cells (HUCPVC): a mesenchymal cell source for dermal wound healing. Organogenesis **6,** 197, 2010.
14. Fischer, C., Schneider, M., and Carmeliet, P. Principles and therapeutic implications of angiogenesis, vasculogenesis and arteriogenesis. Handb Exp Pharmacol **176,** 157, 2006.
15. Zuk, P.A. The adipose-derived stem cell: looking back and looking ahead. Mol Biol Cell **21,** 1783, 2010.
16. Zuk, P.A., Zhu, M., Ashjian, P., *et al.* Human adipose tissue is a source of multipotent stem cells. Mol Biol Cell **13,** 4279, 2002.
17. Levi, B., Wan, D.C., Glotzbach, J.P., *et al.* CD105 protein depletion enhances human adipose-derived stromal cell osteogenesis through reduction of transforming growth factor beta1 (TGF-beta1) signaling. J Biol Chem **286,** 39497, 2011.
18. Jiang, T., Liu, W., Lv, X., *et al.* Potent in vitro chondrogenesis of CD105 enriched human adipose-derived stem cells. Biomaterials **31,** 3564, 2010.
19. Chung, C.G., James, A.W., Asatrian, G., *et al.* Human perivascular stem cell-based bone graft substitute induces rat spinal fusion. Stem Cells Transl Med **3,** 1231, 2014.
20. James, A.W., Zara, J.N., Corselli, M., *et al.* An abundant perivascular source of stem cells for bone tissue engineering. Stem Cells Transl Med **1,** 673, 2012.
21. James, A.W., Zara, J.N., Zhang, X., *et al.* Perivascular stem cells: a prospectively purified mesenchymal stem cell population for bone tissue engineering. Stem Cells Transl Med **1,** 510, 2012.
22. Corselli, M., Chen, C.W., Sun, B., Yap, S., Rubin, J.P., and Peault, B. The tunica adventitia of human arteries and veins as a source of mesenchymal stem cells. Stem Cells Dev **21,** 1299, 2012.
23. Askarinam, A., James, A.W., Zara, J.N., *et al.* Human perivascular stem cells show enhanced osteogenesis and vasculogenesis with Nel-like molecule I protein. Tissue Eng Part A **19,** 1386, 2013.
24. James, A.W., Zara, J.N., Corselli, M., *et al.* Use of human perivascular stem cells for bone regeneration. J Vis Exp e2952, 2012.
25. Saxer, F., Scherberich, A., Todorov, A., *et al.* Implantation of stromal vascular fraction progenitors at bone fracture

sites: from a rat model to a first-in-man study. Stem Cells **34,** 2956, 2016.
26. Wang, J.Y., Zhen, D.K., Falco, V.M., *et al.* Fetal nucleated erythrocyte recovery: fluorescence activated cell sorting-based positive selection using anti-gamma globin versus magnetic activated cell sorting using anti-CD45 depletion and anti-gamma globin positive selection. Cytometry **39,** 224, 2000.
27. Elliot, S., Chalmers, J., and Yang, S. Cell Damage due to Hydrodynamic Stress in Fluorescence Activated Cell Sorters. Ohio State University, 2009.
28. al-Rubeai, M., Emery, A.N., Chalder, S., and Goldman, M.H. A flow cytometric study of hydrodynamic damage to mammalian cells. J Biotechnol **31,** 161, 1993.
29. Llufrio, E.M., Wang, L., Naser, F.J., and Patti, G.J. Sorting cells alters their redox state and cellular metabolome. Redox Biol **16,** 381, 2018.
30. Binek, A., Rojo, D., Godzien, J., *et al.* Flow cytometry has a significant impact on the cellular metabolome. J Proteome Res **18,** 169, 2019.
31. Li, Q., Zhang, X., Peng, Y., *et al.* Comparison of the sorting efficiency and influence on cell function between the sterile flow cytometry and immunomagnetic bead purification methods. Prep Biochem Biotechnol **43,** 197, 2013.
32. Shen, J., Chen, X., Jia, H., *et al.* Effects of WNT3A and WNT16 on the osteogenic and adipogenic differentiation of perivascular stem/stromal cells. Tissue Eng Part A **24,** 68, 2018.
33. James, A.W., Xu, Y., Lee, J.K., Wang, R., and Longaker, M.T. Differential effects of TGF-beta1 and TGF-beta3 on chondrogenesis in posterofrontal cranial suture-derived mesenchymal cells in vitro. Plast Reconstr Surg **123,** 31, 2009.
34. James, A.W., Shen, J., Zhang, X., *et al.* NELL-1 in the treatment of osteoporotic bone loss. Nat Commun **6,** 7362, 2015.
35. Shen, J., James, A.W., Zhang, X., *et al.* Novel Wnt regulator NEL-like molecule-1 antagonizes adipogenesis and augments osteogenesis induced by bone morphogenetic protein 2. Am J Pathol **186,** 419, 2016.
36. Lee, S., Shen, J., Pan, H., *et al.* Calvarial defect healing induced by small molecule smoothened agonist. Tissue Eng Part A **22,** 1357, 2016.
37. Levi, B., James, A.W., Nelson, E.R., *et al.* Human adipose derived stromal cells heal critical size mouse calvarial defects. PLoS One **5,** e11177, 2010.
38. Jackman, C.P., Shadrin, I.Y., Carlson, A.L., and Bursac, N. Human cardiac tissue engineering: from pluripotent stem cells to heart repair. Curr Opin Chem Eng **7,** 57, 2015.
39. Holt, L.M., and Olsen, M.L. Novel applications of magnetic cell sorting to analyze cell-type specific gene and protein expression in the central nervous system. PLoS One **11,** e0150290, 2016.
40. Bareja, A., Holt, J.A., Luo, G., *et al.* Human and mouse skeletal muscle stem cells: convergent and divergent mechanisms of myogenesis. PLoS One **9,** e90398, 2014.
41. Sakaguchi, K., Shimizu, T., Horaguchi, S., *et al.* In vitro engineering of vascularized tissue surrogates. Sci Rep **3,** 1316, 2013.
42. Jia, Z., Liang, Y., Xu, X., *et al.* Isolation and characterization of human mesenchymal stem cells derived from synovial fluid by magnetic-activated cell sorting (MACS). Cell Biol Int **42,** 262, 2018.
43. Wang, Q., Zhang, W., He, G., Sha, H., and Quan, Z. Method for in vitro differentiation of bone marrow mesenchymal stem cells into endothelial progenitor cells and vascular endothelial cells. Mol Med Rep **14,** 5551, 2016.
44. Lv, X.J., Zhou, G.D., Liu, Y., *et al.* In vitro proliferation and differentiation of adipose-derived stem cells isolated using anti-CD105 magnetic beads. Int J Mol Med **30,** 826, 2012.
45. James, A.W., Zhang, X., Crisan, M., *et al.* Isolation and characterization of canine perivascular stem/stromal cells for bone tissue engineering. PLoS One **12,** e0177308, 2017.
46. West, C.C., Hardy, W.R., Murray, I.R., *et al.* Prospective purification of perivascular presumptive mesenchymal stem cells from human adipose tissue: process optimization and cell population metrics across a large cohort of diverse demographics. Stem Cell Res Ther **7,** 47, 2016.
47. Meury, T., Verrier, S., and Alini, M. Human endothelial cells inhibit BMSC differentiation into mature osteoblasts in vitro by interfering with *Osterix* expression. J Cell Biochem **98,** 992, 2006.
48. Zhao, X., Liu, L., Wang, F.K., Zhao, D.P., Dai, X.M., and Han, X.S. Coculture of vascular endothelial cells and adipose-derived stem cells as a source for bone engineering. Ann Plast Surg **69,** 91, 2012.
49. Guillotin, B., Bourget, C., Remy-Zolgadri, M., *et al.* Human primary endothelial cells stimulate human osteoprogenitor cell differentiation. Cell Physiol Biochem **14,** 325, 2004.
50. Guillotin, B., Bareille, R., Bourget, C., Bordenave, L., and Amedee, J. Interaction between human umbilical vein endothelial cells and human osteoprogenitors triggers pleiotropic effect that may support osteoblastic function. Bone **42,** 1080, 2008.
51. Tsang, W.P., Shu, Y., Kwok, P.L., *et al.* CD146+ human umbilical cord perivascular cells maintain stemness under hypoxia and as a cell source for skeletal regeneration. PLoS One **8,** e76153, 2013.
52. Wu, Y.X., Jing, X.Z., Sun, Y., *et al.* CD146+ skeletal stem cells from growth plate exhibit specific chondrogenic differentiation capacity in vitro. Mol Med Rep **16,** 8019, 2017.
53. Gomes, I., Sharma, T.T., Mahmud, N., *et al.* Highly abundant genes in the transcriptosome of human and baboon CD34 antigen-positive bone marrow cells. Blood **98,** 93, 2001.
54. Eridani, S., Sgaramella, V., and Cova, L. Stem cells: from embryology to cellular therapy? An appraisal of the present state of art. Cytotechnology **44,** 125, 2004.
55. de Wynter, E.A., Coutinho, L.H., Pei, X., *et al.* Comparison of purity and enrichment of CD34+ cells from bone marrow, umbilical cord and peripheral blood (primed for apheresis) using five separation systems. Stem Cells **13,** 524, 1995.

Address correspondence to:
Aaron W. James, MD, PhD
Department of Pathology
Johns Hopkins University
Ross Research Building
Room 524A
720 Rutland Avenue
Baltimore, MD 21205

E-mail: awjames@jhmi.edu

Received: February 6, 2019
Accepted: April 12, 2019
Online Publication Date: August 15, 2019